1996ApJ...462..768U

THE ASTROPHYSICAL JOURNAL, 462:768–776, 1996 May 10
© 1996. The American Astronomical Society. All rights reserved. Printed in U.S.A.

A CANDIDATE ENERGY SOURCE FOR THE GALACTIC CENTER NONTHERMAL FILAMENT G359.1−0.2, "THE SNAKE"

KEVEN I. UCHIDA
Max-Planck-Institut für Radioastronomie, Auf dem Hügel 69, 53121 Bonn, Germany
MARK MORRIS
Division of Astronomy, Department of Physics and Astronomy, University of California, Los Angeles, CA 90095-1562
E. SERABYN
Department of Physics, 320-47, California Institute of Technology, Pasadena, CA 91125
AND
ROLF GÜSTEN
Max-Planck-Institut für Radioastronomie, Auf dem Hügel 69, 53121 Bonn, Germany
Received 1995 April 24; accepted 1995 October 27

ABSTRACT

We report the discovery of an H II region/molecular cloud complex toward the northern extreme of the Galactic center nonthermal filament G359.1−0.2, also known as the "Snake." The ^{12}CO and ^{13}CO molecular emission, observed with the 10.4 m antenna of the Caltech Submillimeter Observatory, arises from several massive clumps situated near one end of the Snake and surrounding the H II complex. The high velocities (−180 to −100 km s^{-1}) and large line widths (25–50 km s^{-1}) of the molecular emission are characteristic of gas within the Galactic center region. Moreover, the systematically arranged velocities of the individual molecular clumps imply that they belong to a common kinematic system.

Association between the cloud, the filament, and the H II region is suggested by the data. An anticorrelation between the filament and the molecular emission, where the filament is superposed on the cloud, is attributed to interaction between the two. The H79α recombination line, observed with the 100 m Effelsberg antenna toward the H II complex, is centered at a velocity (−180 km s^{-1}) similar to that of the surrounding molecular gas.

By revealing a candidate energy source for one of the nonthermal Galactic center radio filaments, this study provides support for the hypothesis that these filaments are manifestations of strong vertical field lines (of mG strength) illuminated by the magnetohydrodynamic response to a collision with a magnetized molecular cloud. According to this hypothesis, reconnection of magnetic field lines at an ionized cloud surface is responsible for acceleration of electrons to relativistic velocities along the filament. Ionization of the cloud by a centrally located stellar source provides a copious supply of free electrons. While the requisite elements of this mechanism are in evidence at one end of G359.1−0.2, the details of the hypothesized interaction have yet to be confirmed.

Subject headings: Galaxy: center — H II regions — ISM: individual (G359.1−0.2) — radio lines: ISM

1. INTRODUCTION

The Galactic center region contains a number of unusual thermal and nonthermal radio sources, the most notable of which is a group of features known as the "filaments" or "threads" (Yusef-Zadeh 1989; Morris 1990). As their name implies, the filaments are approximately linear; they range between 5′ and ∼20′ in length (between 12 and 50 pc if a Galactic center distance of 8.5 kpc is adopted) but are less than several arcseconds in width. All the filaments are oriented approximately perpendicular to the Galactic plane and produce highly polarized nonthermal emission. The Galactic center radio arc (GCRA), probably the best known of all the filamentary structures, is the most complex and elaborate of such systems, with both thermal and nonthermal components (Yusef-Zadeh, Morris, & Chance 1984; Yusef-Zadeh & Morris 1987a; Morris & Yusef-Zadeh 1989). To date, about seven filaments, or filament groups, have been detected within a 1° radius of the Galactic center (Anantharamaiah et al. 1991; Morris 1995b).

The nonthermal filaments are believed to be the manifestations of strong vertical field lines (≥1 mG) which are either contained in localized bundles (Yusef-Zadeh & Morris 1987a; Serabyn & Güsten 1991; Uchida & Güsten 1995) or which are perhaps permeating the entire 200 pc radius Galactic center region (Morris 1990, 1995a; Sofue 1990). The filaments represent magnetic flux tubes into which synchrotron-radiating relativistic particles have been injected. Indeed, radio polarization measurements show that the implied magnetic field follows the filaments (Tsuboi et al. 1985, 1986; Yusef-Zadeh et al. 1995). Just how these particular field lines are chosen for illumination, however, is somewhat less clear. In several cases, a molecular cloud is observed situated along the edge, or at the end, of a nonthermal filament. High-resolution CS (J = 2–1) single-dish maps taken by Serabyn & Güsten (1991) and interferometric images by Serabyn & Morris (1994) provide strong evidence (both morphological and kinematic) of an association between a +25 km s^{-1} molecular cloud and an extended ionized region intimately associated with the nonthermal filaments of the GCRA (Yusef-Zadeh & Morris 1987b). This has led to various hypotheses regarding the origin of the filamentary structures. First, it was suggested that a large relative velocity between the cloud and the ambient field may be responsible for either the surficial ionization of the cloud, or the accerleration of the particles to relativistic energies, or both, as a result of an induced electric field

© American Astronomical Society • Provided by the NASA Astrophysics Data System

1996ApJ...462..768U

(Benford 1988; Morris & Yusef-Zadeh 1989). Magnetic field line reconnection at cloud/field interfaces was also considered as a means of accelerating particles (Heyvaerts, Norman, & Pudritz 1988; Serabyn & Güsten 1991; Lesch & Reich 1992; Serabyn & Morris 1994). Most recently, Serabyn & Morris (1994) have argued that the production of synchrotron filaments is caused by magnetic field line reconnection at the cloud/field interface, but that two conditions must be met: first, a magnetized cloud, or a magnetized clump within a cloud, must move with sufficiently high velocity (preferably a velocity well in excess of the cloud's internal velocity dispersion) with respect to the ambient external field. Second, the cloud surface must be ionized, so that an ample supply of free electrons is present and available for acceleration when field line reconnection takes place. The ionization is presumably accompanied by turbulent mixing of cloud material at the interface, guaranteeing a replenishment of cloud magnetic field at the surface. The surface ionization could, in principle, be the result of the critical ionization phenomenon (Morris & Yusef-Zadeh 1989; Nicholls 1992), but for the GCRA, UV ionization by stellar sources is strongly in evidence.

G359.1−0.2, known as the "Snake," is the most recently discovered Galactic center nonthermal filament (Gray et al. 1991, 1995). It is highly polarized, by as much as 60% at some locations (Reich & Schlickeiser 1992), and its mean spectral index, α, is -0.2 ± 0.2, where $S = \nu^{\alpha}$, although α may vary from -0.8 to ~ 0.2 from the southern to the northern extremities of the Snake (Gray et al. 1995). This filament extends south from the Galactic plane for a little more than 20′ (Fig. 1*a*), or 50 pc, to where it crosses the nonthermal Galactic center shell G359.1−0.5 (Uchida et al. 1992a). There has been speculation of an association between the two; a $\lambda 20$ cm absorption-line study of this region done by Uchida, Morris, & Yusef-Zadeh (1992b) constrains the nonthermal shell and filament to within a few hundred parsecs of one another, at the distance to the Galactic center. In addition, in the $\lambda 21$ cm continuum images, there is a distinct brightening in the nonthermal shell (and a flattening of the shell's spectral index; Gray 1994) where the filament crosses its perimeter, perhaps manifesting an input of energy from the filament into the shell. Gray et al. (1995) suggest a slight bending of the Snake filament at the point of intersection with the expanding G359.1−0.5 shell, but this could simply be one of the "kinks" in this unusual filament. Indeed, a much more pronounced bending would be expected if the magnetic field lines were subjected to the large ram pressure of a supernova shell. It is not clear that it is even possible for a magnetic filament to penetrate relatively unscathed into the interior of a supernova remnant, as the Snake appears to do if the superposition is not merely owed to projection.

Toward the northern tip of the Snake filament is another candidate for association: a cluster of H II knots, G359.19−0.05 (Caswell & Haynes 1987) about which little is known to date. This H II complex is the subject of the multiwavelength study presented here, the goal of which was (1) to investigate the possibility that the "Snake" nonthermal filament is associated with the G359.19−0.05 H II complex, (2) to determine whether a molecular cloud is implicated in the association, and (3) to gather evidence which may shed light on the applicability of the magnetic reconnection hypothesis to the illumination of the Snake. The latter goal has yet to be realized, although we can now argue that the requisite elements for this mechanism are present.

2. OBSERVATIONS

2.1. *Molecular Line Observations*

The ^{12}CO $J = 2$–1 and the ^{13}CO $J = 2$–1 transitions were observed between 1992 August 1–3 with the 10.4 m antenna of the Caltech Submillimeter Observatory (CSO). The HPBW of the telescope at the transition frequency of the ^{12}CO $J = 2$–1 line (230 GHz) was 30″. A pointing uncertainty of approximately $\pm 3''$ was achieved by periodically centering the antenna on the peak signal from Jupiter. The receiver front end was a waveguide-mounted SIS receiver. An acousto-optical spectrometer with 1024 channels and a frequency coverage of 500 MHz comprised the back end. The total velocity coverage for the ^{12}CO observations, centered on $V_{\rm LSR} = 0$ km s^{-1}, was ± 325 km s^{-1}, and the velocity resolution was about 1.3 km s^{-1}.

The ^{12}CO observations presented in this paper comprise a complete 8′ × 10′ grid, centered on the H II complex, with 15″ spacing between observations in right ascension and 30″ spacings in declination. The average on-time integration for each spectrum was 90 s, resulting in an rms noise level of about 0.3 K. The ^{13}CO observations were taken toward selected regions extending over approximately a third of the area covered by the ^{12}CO grid. All the observations were taken using the CSO "on-the-fly" continuous mapping procedure, with the off-position for each R.A. strip located at $\alpha, \delta_{(1950)} = (17^{\rm h}43^{\rm m}33^{\rm s}.24, -30°14'25'')$, a nearby position relatively far from the Galactic plane and free of any high-velocity CO line emission.

2.2. *Continuum Observations*

The 20 and the 3.6 cm continuum images in Figure 1 were taken as part of a study of the G359.1−0.5 supershell region (Uchida et al. 1992b) performed on 1991 February 15 and 18 with the DnC configuration of the Very Large Array (VLA)[1]. The 20 cm data comprise a nearly full set of visibilities, whereas the 3.6 cm data are a "snapshot" of ∼15 minutes duration. The 3.6 cm image was produced using natural weighting of the visibility data, and the 20 cm image was produced with uniform weighting; the resulting clean beam sizes are 9″.1 × 7″.7 (P.A. = 72°.2) and 32″.7 × 30″.8 (P.A. = −56°.1), respectively. We refer to Uchida et al. (1992b) for additional details of the 20 cm observations and image production.

2.3. H79α *Recombination Line Observations*

The H79α recombination line (13.08 GHz) was observed on 1994 February 16 and 17 with the 100 m antenna of the MPIfR located near Effelsberg, Germany. The HPBW of the antenna was 65″, and a pointing accuracy of better than 10″ was achieved by scanning across the continuum source NRAO 530. The front end system consisted of a dual channel receiver, with HEMT preamplifiers, measuring the two senses of circular polarization. The left and right circularly polarized spectral components were summed during the postobserving stage. A 25 MHz bandwidth was sampled

[1] The VLA is a facility of the National Radio Astronomy Observatory, which is operated by Associated Universities, Inc., under cooperative agreement with the National Science Foundation.

© American Astronomical Society • Provided by the NASA Astrophysics Data System

1996ApJ...462..768U

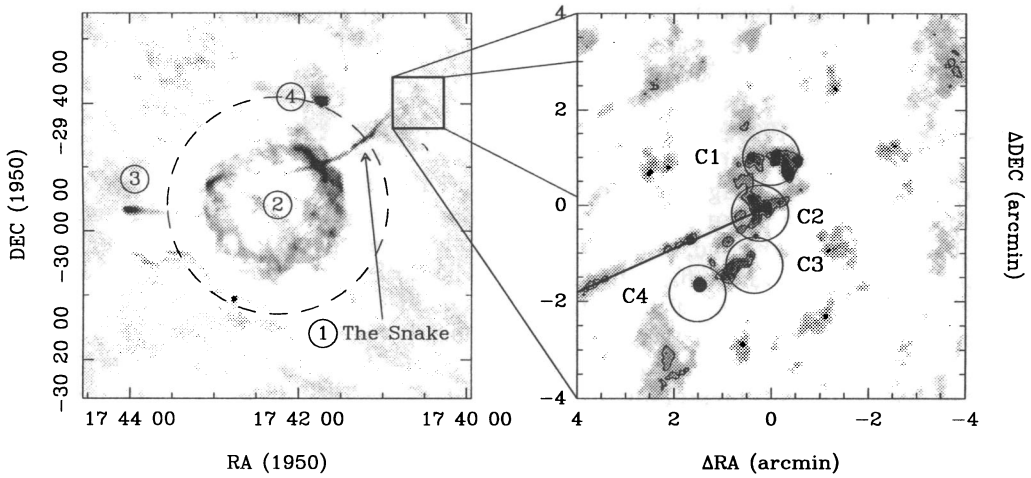

FIG. 1.—*Left*: A 21 cm VLA continuum image of (1) the nonthermal GC filament G359.1−0.2, the "Snake." Also in the field are (2) G359.1−0.5, a GC superbubble/supernova shell, (3) G359.2−0.8, an unusual continuum source with a cometary tail, and (4) G359.28−0.26, an H II region with bow shock morphology. The G359.19−0.05 H II complex at the northern end of the Snake (position indicated by the box) is not seen in the 21 cm image because it is both weak and is well outside the FWHP primary beamwidth (34′) of the VLA at this wavelength (indicated by the dashed circle). *Right*: A 3.6 cm continuum snapshot of G359.19−0.05, the cluster of H II regions at the northern end of the Snake. The sizes of the circles correspond to the FWHM beamwidth (65″) of the 100 m antenna at the transition frequency of H79α. The filamentary Snake is indicated by the solid line. The map offsets are with respect to the central position α, $\delta_{(1950)}$ = ($17^h40^m35^s.0$, −29°40′00″).

with a 512 channel autocorrelator, providing a velocity resolution of 1.1 km s^{-1}. The velocity coverage was between −361 and 211 km s^{-1}, centered on V_{LSR} = −75 km s^{-1}.

Four positions were observed among the various continuum peaks toward G359.19−0.05; they are identified as C1 through C4 in Figure 1 (*right*). Integration times ranged between a maximum of 64 minutes toward position 1 and a minimum of 7 minutes on position 3, resulting in rms noise values of between 15 mK and 43 mK in the unsmoothed spectra. The observations were performed by position switching; the off-position was located at α, $\delta_{(1950)}$ = ($17^h48^m54^s.54$, −28°54′01″), a nearby position found free of H79α line emission. The average system temperature during the observations was approximately 35 K.

3. RESULTS

3.1. *Continuum Images and Recombination Line Data*

The left-hand panel of Figure 1 is a 20 cm continuum image which includes the nonthermal filament known as the Snake, as well as a number of other remarkable continuum features. The Snake extends from the approximate center to the upper right corner of the image; it crosses G359.1−0.5, the supernova remnant/supershell located at the distance to the Galactic center (Uchida et al. 1992a, b). East of the nonthermal shell is G359.2−0.8, a nonthermal source with a cometary morphology (Yusef-Zadeh & Bally 1989), located foreground ($d < 5$ kpc) to the Galactic center (Uchida et al. 1992b).

The right-hand panel of Figure 1 details the 3.6 cm continuum emission toward the northern end of the nonthermal filament. The map offsets are with respect to the central position α, $\delta_{(1950)}$ = ($17^h40^m35^s.0$, −29°40′00″). Hereafter, all the spatial maps presented are centered on and all offsets quoted are with respect to this position. The Snake is not well characterized in the 3.6 cm image, appearing only as a line of emission clumps, because of the relatively poor sensitivity (0.1 mJy $beam^{-1}$ rms) of this "snapshot" image and because the emission from the Snake itself is relatively weak near its northern tip. Nevertheless, it extends at least to Δα, Δδ = (0′, 0′), the approximate center of the H II complex (see Fig. 2 of Gray et al. 1995). The peak intensity from the portion of the Snake contained in our images is 0.5 Jy $beam^{-1}$ (at Δα, Δδ = 1′.7, −0′.7).

The 3.6 cm image details a number of compact sources interspersed within a diffuse emission component. The strongest continuum source is observed toward position C4; its emission, characterized with a spectral index (α) of 1.2 (where $S = \nu^{-\alpha}$), appears to be nonthermal (Leahy 1991b). The C4 continuum source was first suggested by Leahy (1991a) to be the radio counterpart to 1E 1740−2942, the strongest compact source of 511 keV electron-positron annihilation line radiation observed toward the Galactic center and candidate for an accreting black hole (Mirabel et al. 1991, 1992). However, observations by the *Granat* satellite have since shown 1E 1740−2942 to lie a little more than 2′ south of the continuum point source C4 (Paul et al. 1991). The remaining weaker and more diffuse components of 3.6 cm emission, which we attribute to the G359.19−0.05 H II complex, are observed toward positions C1, C2, and C3. Like the weak extended emission from the Snake, they are also poorly characterized (especially those toward positions C2 and C3) because of the low sensitivity of the image. Moreover, any thermal emission toward position C2 may be confused with the nonthermal continuum emission arising from the superposed Snake.

An unpublished 6 cm image, made by Echevarria (1995), shows extended emission toward the G359.19−0.05 region apparently resolved out by our λ = 3.6 cm observations. The 6 cm emission extends almost continuously over a 4′ × 2′.5 elliptical region, centered on α, $\delta_{(1950)}$ = ($17^h40^m34^s$, −29°39′00″) and containing the positions C1–C3. The excitation parameter, found from the 6 cm flux integrated over the entire region (0.35 Jy), is 33 pc cm^{-2} at the 8 kpc distance of the Galactic center, corresponding to a single O9 V central ionizing star. That a single star can account for this H II region is ascribable to its modest density. With a mean emission measure of 2×10^3 pc cm^{-6} and an assumed depth of 5 pc, the rms electron density is only 20 cm^{-3}.

© American Astronomical Society • Provided by the NASA Astrophysics Data System

1996ApJ...462..768U

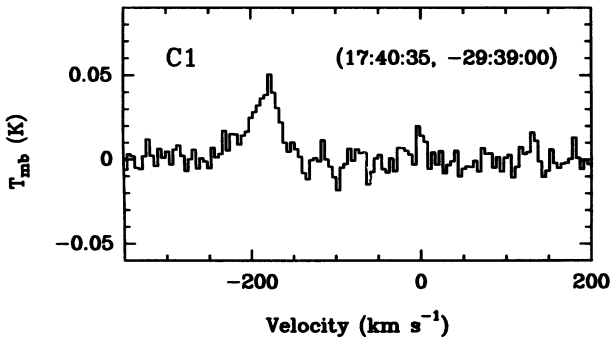

FIG. 2.—H79α recombination line spectrum toward the continuum position C1 indicated in Fig. 1*b*.

The H79α observations reveal a 41 mK line toward position C1, $\Delta\alpha$, $\Delta\delta = (0', 1')$, centered at $V_{LSR} = -183$ km s^{-1} and with a full, half-maximum velocity width of 40 km s^{-1} (Fig. 2). The large radial velocity of this emission indicates that it likely arises from a Galactic center source. No emission is seen toward the remaining positions above a 2 σ limit of ∼9 mK (with the spectra smoothed to a resolution of 40 km s^{-1} channel^{-1}).

3.2. *Molecular Line Data*

An inspection of the ^{12}CO channel maps reveals that emission at velocities overlapping that of the H76α line is localized around the H II region and the northern tip of the Snake. Figure 3 is a gray-scale map of the ^{12}CO emission, integrated between −200 and −78 km s^{-1}, superposed upon the 3.6 cm continuum contour map of the Snake and H II cluster. The most prominent molecular peaks are observed distributed in a ∼4′ diameter patchy ringlike structure centered on $\Delta\alpha$, $\Delta\delta = (0'.25, -1'.5)$ and encircling the G359.19−0.05 H II complex. A close physical association between the H II region and the surrounding molecular gas is implied. It is noteworthy that there is a distinct minimum in the ^{12}CO emission where the Snake crosses the eastern perimeter of the molecular "ring" ($\Delta\alpha$, $\Delta\delta = 1'.75$, $-0'.75$).

Figure 4*a*, a ^{12}CO spectrum centered on position C1 ($\Delta\alpha$, $\Delta\delta = 0$, 1′), displays a complex blend of spectral com-

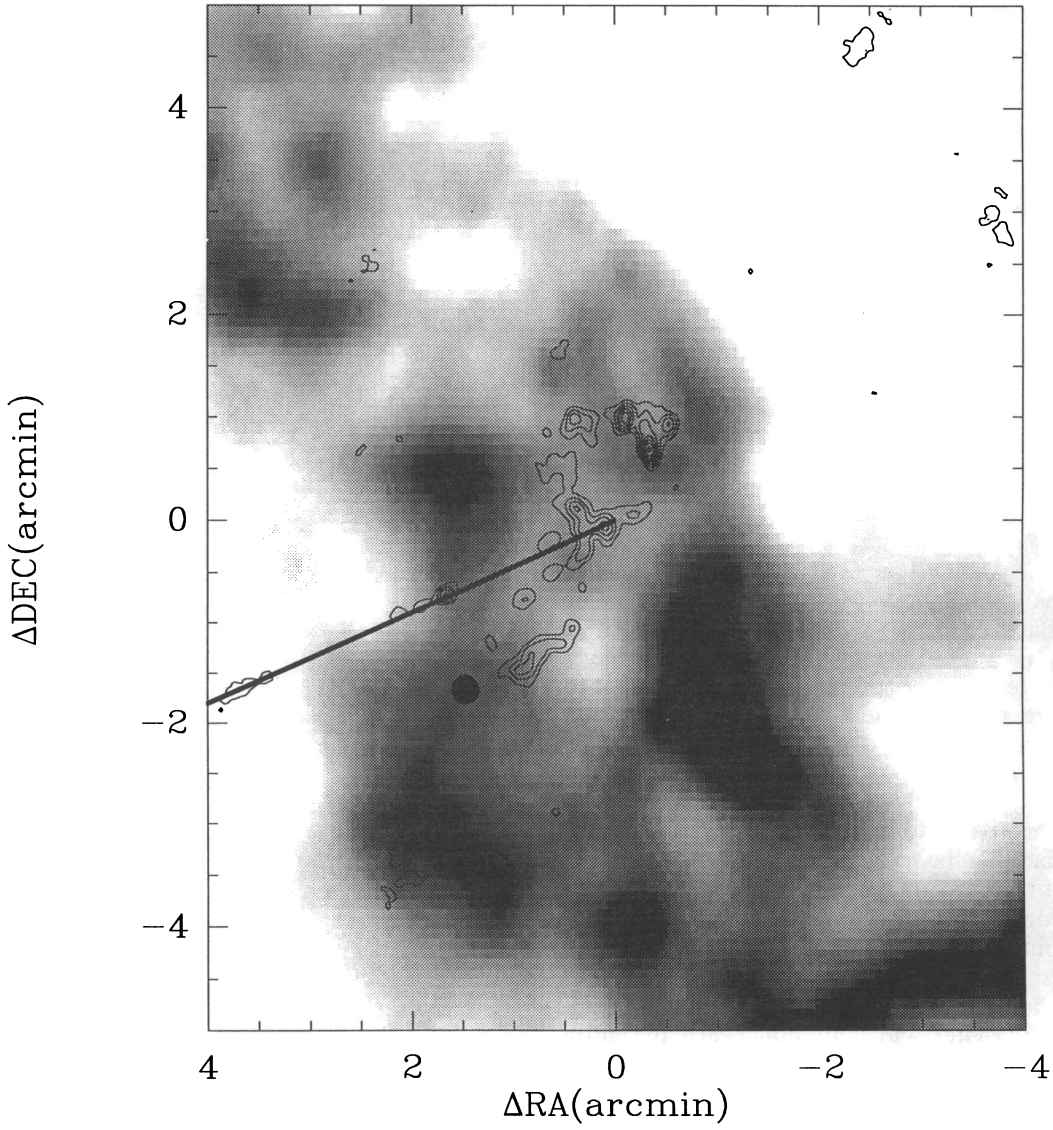

FIG. 3.—A 3.6 cm VLA continuum image (*contours*) of the G359.19−0.05 region superposed upon a gray-scale image of ^{12}CO $J = 2$–1 emission integrated between $V = -200$ and -78 km s^{-1}. The contour levels extend between 4.5×10^{-4} and 9.0×10^{-2} in increments of 2.0×10^{-4} Jy beam^{-1}.

© American Astronomical Society • Provided by the NASA Astrophysics Data System

1996ApJ...462..768U

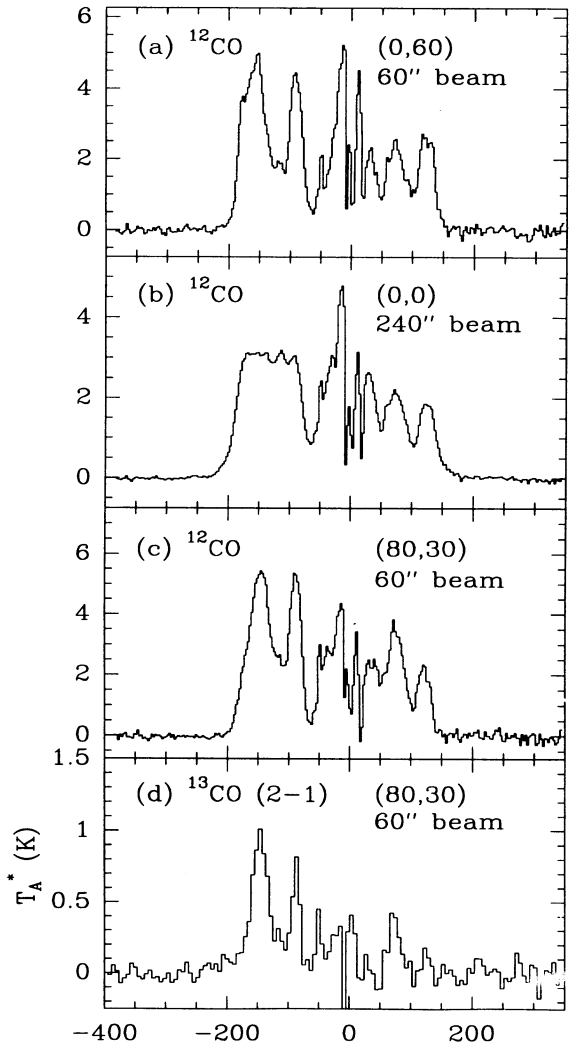

FIG. 4.—The ^{12}CO $J = 2$–1 spectra convolved to (*a*) a 60″ Gaussian beam centered on $\Delta\alpha, \Delta\delta = (0'', 60'')$, (*b*) a 240″ Gaussian beam centered on $\Delta\alpha, \Delta\delta = (0'', 0'')$, and (*c*) a 60″ Gaussian beam centered on $\Delta\alpha, \Delta\delta = (80'', 30'')$. (*d*) The ^{13}CO $J = 2$–1 spectra convolved to a 60″ Gaussian beam centered on $\Delta\alpha, \Delta\delta = (80'', 30'')$.

ponents at high negative velocities. The high velocities and large line widths of this gas place it within the Galactic center region (Bally et al. 1987, 1988). The high positive velocity emission ($V = 50$–150 km s^{-1}), although also likely to be Galactic center gas, does not appear to be localized to this particular region. The near-zero velocity emission ($<|50|$ km s^{-1}) is attributed to gas located in either the foreground or the background of the Galactic center region.

The individual ^{12}CO and ^{13}CO spectra show the high negative velocity emission to be a blend of several spectral components rather than being a single self-absorbed profile. The velocities of the individual components vary considerably with position; over the region studied, gas is present over almost a continuous range of velocities between -210 and -70 km s^{-1}. This is illustrated in Figure 4*b*, a ^{12}CO spectrum from the data convolved to a 4′ Gaussian beam, centered on the grid center, and containing nearly the entire molecular ring shown in Figure 3.

The spectrum in Figure 4*c* was produced from the ^{12}CO data, convolved to a 1′ beam centered on $\Delta\alpha, \Delta\delta = (0.8', 0.5')$, the location of one of the prominent molecular clumps bordering the H II complex. The ^{13}CO $J = 2$–1 spectrum was also observed over this subregion and is shown in Figure 4*d*. The ^{12}CO optical depth, determined from the ^{12}CO/^{13}CO line ratio (with an assumed isotopic ratio of 25; Wannier 1989, Henkel et al. 1983), is ~ 5. Thus, assuming a kinetic temperature of ~ 50 K for gas in the Galactic center region (Morris et al. 1983) and given a measured peak temperature of only 5.5 K for the ^{12}CO $J = 2$–1 line (Fig. 4*c*), we note that the ^{12}CO gas appears to either have a low beam filling factor, or, more likely, a subthermal excitation in the surface layer of the cloud because of the relatively low densities there.

Figure 5 contains gray-scale images of the integrated ^{12}CO emission in three velocity ranges. Superposed on all three images is the 3.6 cm VLA image of the region. An apparent anticorrelation between the continuum and molecular components is found in all three frames (i.e., the molecular emission is exclusive of, but closely borders, the H II region), perhaps implying interaction between the two. The highest negative-velocity component in Figure 5 (*top*) is

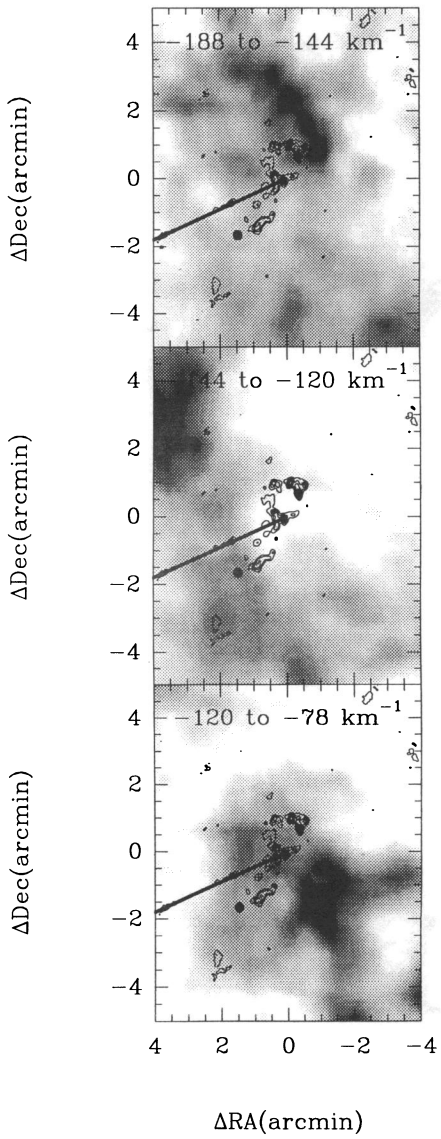

FIG. 5.—A 3.6 cm contour map of the G359.19−0.05 H II region superposed with gray-scale images of ^{12}CO $J = 2$–1 emission integrated between (*top*) $V = -188$ and -144 km s^{-1}, (*middle*) $V = -144$ and -120 km s^{-1}, and (*bottom*) $V = -120$ and -78 km s^{-1}.

© American Astronomical Society • Provided by the NASA Astrophysics Data System

1996ApJ...462..768U

localized mainly in the northern half of the image. There the molecular emission is found along a ridge extending from $\Delta\alpha, \Delta\delta = (-1'.0, 0'.75)$—a position lying along a line extending from the Snake—to $\Delta\alpha, \Delta\delta = (1'.5, 3'.0)$. The southern edge of the molecular "ridge" borders the continuum peaks at position C1. The molecular ridge appears weakly, if not incompletely, in Figure 3, as the gray-scale range of that image was set to display the other, more prominent emission components.

The strongest emission at intermediate velocities (Fig. 5 [*middle*]) is localized at the northeastern edge of the field. Much of the remaining intermediate-velocity emission, which is more diffuse in nature, is distributed throughout the southern half of the panel. The entire H II complex, with exception of the southern portion toward position C4, is contained in a local minimum of the diffuse CO component at intermediate velocities. The boundary between the molecular gas and the radio continuum emission is best defined along the eastern and southern border of the H II complex.

Figure 5 (*bottom*) displays the strongest anticorrelation between the 3.6 cm continuum and molecular component among the three velocity ranges. The -120 to -78 km s^{-1} gas is peaked at the positions $\Delta\alpha, \Delta\delta = (-1'.0, -1'.5)$ and $(1'.0, 0'.0)$, toward either side of the diagonally elongated H II complex.

Figure 6, a series of channel maps in velocity increments of 5.7 km s^{-1}, shows a large-scale spatial trend in the ^{12}CO velocities. The ^{12}CO emission appears to move in an elliptical pattern counterclockwise around the approximate map center with progression from the highest negative velocity panels to the lowest. An ellipse is superposed to illustrate this point. The highest velocity emission ($V = -181$ km s^{-1}) first appears at about 1′ northwest of the map center (indicated by the cross). The emission then proceeds counterclockwise along the elliptical trace until it reaches a velocity of about -95 km s^{-1}; note especially the correspondence of the gas to the elliptical shape at $V = -163.9$ and -158.1 km s^{-1}. At the low-velocity extreme ($V > -95$ km s^{-1}), the emission falls interior to the ellipse.

The kinematical structure implied by this scenario cannot be easily ascribed to simple ring expansion or rotation; the data may instead be indicative of more complicated nonplanar motions. Figure 7 (*top*) is a position-velocity diagram constructed from spectra taken from positions (Fig. 7, *bottom*) around the gaseous "ellipse." The values along the position axis in the top panel refer to the point labels in the lower finder image. The points were selected to be approximately equidistant along the elliptical pattern. The high negative-velocity emission in Figure 7 (*top*) extends continuously across the entire positional extent of the map. The strongest component of that emission, which is concentrated in a diagonal band across the diagram, decreases steadily in velocity from about -180 km s^{-1} at position 1 to about -100 km s^{-1} at position 12. The only deviation from a steady decrease in the negative gas velocities around the position-velocity map occurs beyond posi-

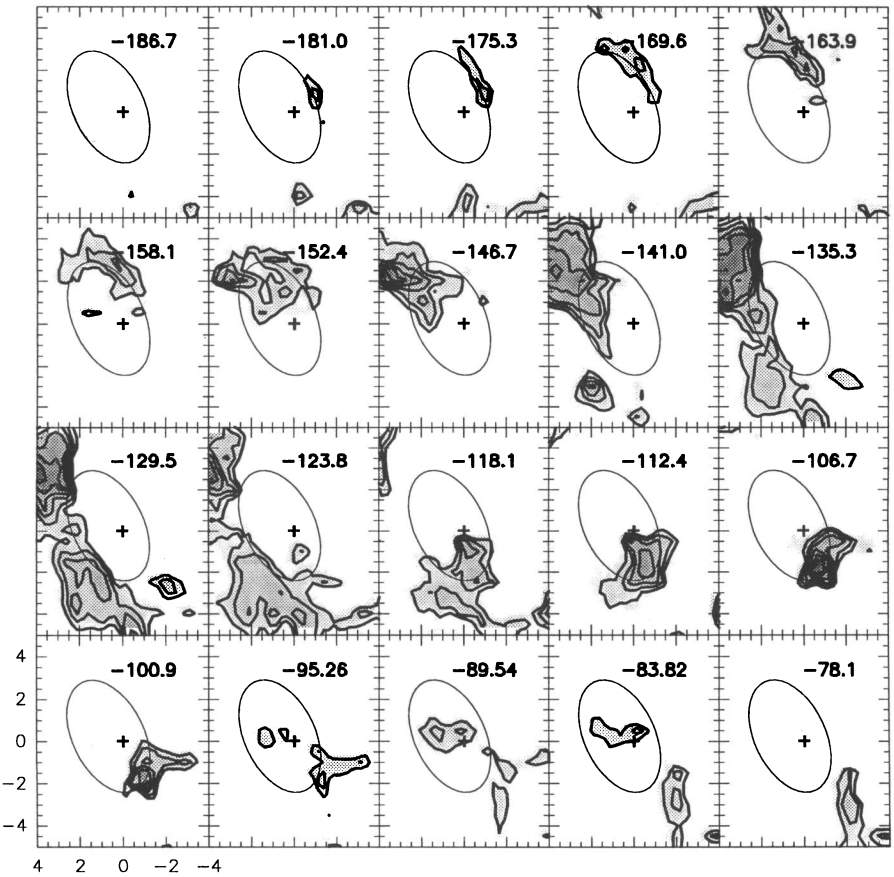

FIG. 6.—Channel maps of ^{12}CO $J = 2$–1 emission spaced in velocity increments of $+5.7$ km s^{-1}. The contour levels are $T_A^* = 5$–15 K in increments of 1 K. The cross marks the center of the map. The superposed ellipse is centered at $\Delta\alpha, \Delta\delta = (40'', 15'')$, has a major axis length of 170″ and a minor axis length of 100″, and is oriented at a position angle of 25°.

© American Astronomical Society • Provided by the NASA Astrophysics Data System

1996ApJ...462..768U

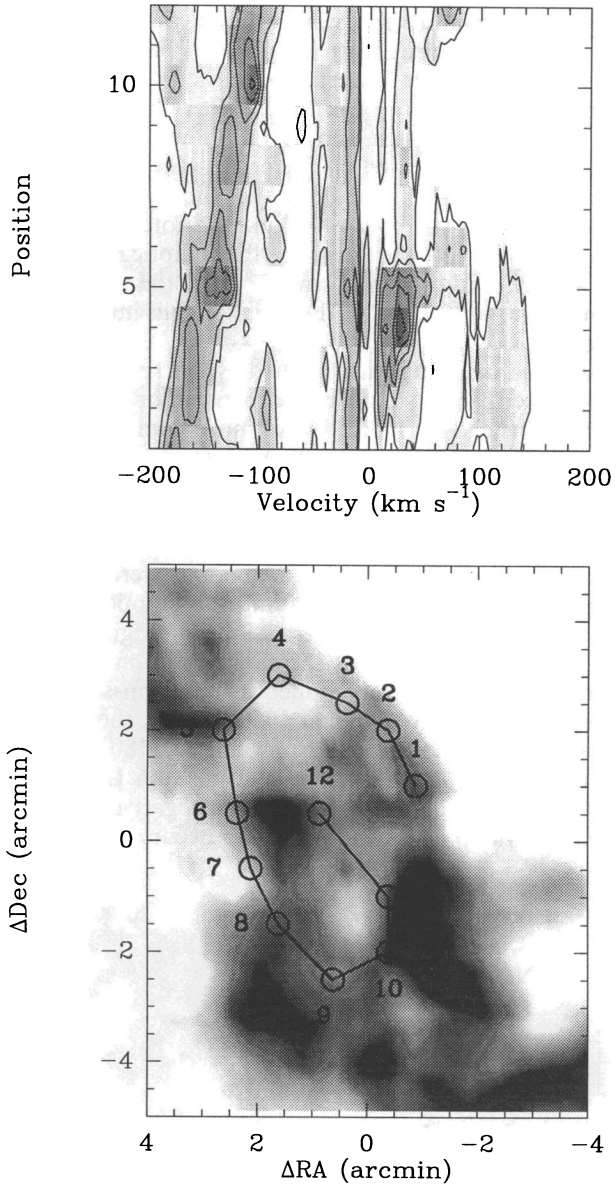

FIG. 7.—*Top*: Position-velocity diagram of ^{12}CO emission constructed from spectra toward the 12 positions shown in the bottom panel. The numbering along the position axis corresponds to the point identifications in the lower panel. The contour levels are from $T_A^* = 2$ to 20 K in increments of 2 K.

tion 8, where the emission branches into two velocity components. There the lowest level contours gradually extend back to the high negative velocities (-180 km s^{-1}) originally observed at position 1. The partial sinusoidal pattern formed by the high negative-velocity emission from positions 1–8, and the relatively weak emission in the highest velocity branch from positions 9–12 (2–4 K) could be accounted for by an expanding, tilted ring structure. However, it cannot be ruled out that the weak high-velocity emission between positions 9 and 12 is from an unassociated, superposed component.

An alternative interpretation of the apparent molecular ring is that it is a chance superposition of two cloud systems, one which dominates the northern sector and is present between -181 and -118 km s^{-1}, shows a consistent velocity gradient of about 12 km s^{-1} arcmin^{-1} from west to east (see Fig. 6), and curls around, or avoids, the H II region. The other cloud system is present in the southern half of the complex. It first appears as a pronounced clump at -141 km s^{-1} at $(\Delta\alpha, \Delta\delta) = (2', -3')$ and progresses westward toward increasing velocities, also appearing to curl around the H II region in the south. Its velocity gradient, of ~ 11 km s^{-1} arcmin^{-1} from east to west, is in the opposite sense to the northern cloud. The link between the two systems (at [2′, 0′] in the -135 km s^{-1} to -124 km s^{-1} panels) is not obviously a continuous, physical one. The hypothesis of two separate cloud systems would help account for the emission continuing out of the region mapped to the northeast (for the northern complex) and to the southwest (for the southern complex). Under this hypothesis, the H II region might be accounted for in terms of star formation at the interface between colliding clouds, but this leaves open the question of why two systems with unusually large velocity gradients in opposite senses should be located so close to each other.

The clump appearing at about (2′, −3′) in the −141 km s^{-1} channel warrants particular attention. It corresponds to the molecular clump which has been associated with the γ-ray source 1E 1740.7−2942, the so-called Great Annihilator (Mirabel et al. 1991; Bally & Leventhal 1991). These papers suggest the hypothesis that the high-energy source is powered by accreting matter directly out of the molecular cloud. Contours of the radio emission from 1E 1740.7−2942 (see Mirabel et al. 1992) can be seen weakly in Figures 1 and 3. The molecular data presented here show that the superposed and potentially associated molecular clump is part of the system surrounding the G359.19−0.05 H II region, or is at least a component of the southern complex. It therefore places this clump in a larger context.

3.3. *The Mass of the Molecular Material about G359.19−0.05*

An order-of-magnitude mass estimate for the molecular "ring" was made using the integrated CO line intensity of H_2 column density conversion factor, $N(H_2)/I_{CO(1-0)} = 2.8 \times 10^{20}$ cm^{-2} (K km s^{-1})$^{-1}$, determined empirically by Bloemen et al. (1986). The conversion factor was applied to the integrated ($V = -200$ to -75 km s^{-1}) ^{12}CO $J = 2$–1 emission map; the total gas mass, determined from the summed contributions of all pixels above the 20% level in the map, is 6×10^5 $M_\odot$. This result is likely an overestimate, however, because of the fact that we have used the integrated ^{12}CO $J = 2$–1 line intensities rather than those of the $J = 1$–0 transition as prescribed by the relation. Given the mean ^{12}CO optical depth of ~ 5 inferred from the measured ^{13}CO/^{12}CO line ratios, the integrated ^{12}CO (2–1)/(1–0) ratio is further constrained to within ~ 2 for the range of physical conditions and kinetic temperatures considered reasonable for the Galactic center region (T_{kin} = 40–80 K), this determined by means of a statistical line modeling code (with large velocity gradient assumption). Therefore, we estimate the total mass of the "ring" to be within the range of 3–6×10^5 $M_\odot$. This implies a total internal kinetic energy of $\sim 10^{51}$ ergs for the ring.

The ^{13}CO line observations, in conjunction with those of ^{12}CO, provide another means by which to determine the total gas column densities toward the G359.19−0.05 region. Because of the limited ^{13}CO coverage, however, we were unable to determine the mass over the entire molecular "ring" by this method. Instead, the mass determinations are limited to 0.5 radius regions, centered on the peaks of

© American Astronomical Society • Provided by the NASA Astrophysics Data System

1996ApJ...462..768U

two prominent clumps located east of the H II region. With the $\tau(^{13}CO)$ inferred from the $^{12}CO/^{13}CO$ ratio, and assuming a $^{12}CO/H_2$ mass ratio of $8.5 \pm 2.3 \times 10^{-5}$ (Frerking, Langer, & Wilson 1982), we determine total masses of $4–7 \times 10^3\ M_\odot$ and $3–6 \times 10^3\ M_\odot$ for the clumps located at $\Delta\alpha, \Delta\delta = (80'', 30'')$ and $(105'', -180'')$, respectively; the ranges quoted allow for a possible enhancement of the $^{12}CO/H_2$ mass ratio in the Galactic center region by up to a factor of 2, reflecting the probably enhanced metallicity there. These masses compare well to the $3–7 \times 10^3$ and $4–9 \times 10^3\ M_\odot$ determined for the same clumps using the integrated ^{12}CO line intensities. The masses derived from isotope ratios should be approached with caution, however, for the usual reasons that clumping within the cloud will enhance the $^{12}CO/^{13}CO$ intensity ratio and lead to an underestimate of τ, while subthermal excitation in the outer, low-density layers of a cloud, where the ^{12}CO line first becomes optically thick, will depress the observed $^{12}CO/^{13}CO$ ratio and lead to an overestimate of τ.

4. DISCUSSION

4.1. *The G359.1−0.5 H II Region and the Snake*

The observations presented here provide evidence that the G359.19−0.05 H II complex is associated with the surrounding molecular medium, which apparently takes the form of a broken "ring" of molecular gas. The apparently continuous trend in velocities along the perimeter of the ring suggests that much or all of the molecular gas is part of a single kinematic feature. Despite, however, the projected appearance of the gas as a ring, the velocity trends are inconsistent with both simple expansion and rotation by such a feature, indicating that the actual three-dimensional gas distribution is more complicated. It seems likely that the ionized gas is in a blister-type configuration, where the stellar sources are in the process of disrupting the cloud. The H79α line emission from source C1 in G359.19−0.05 ($V = -185$ km s^{-1}) is blueshifted with respect to most of the molecular gas at that location, which suggests that the H II region is streaming toward us off of the near edge of the molecular complex. The extremely low density of the H II region (rms value of 20 cm^{-3}) implies that the center of the molecular ring is essentially empty, and that the ionized gas is able to expand unhindered off the molecular cloud surface. A higher resolution view of the molecular emission is now needed to determine the velocity of the molecular clump associated with H II source C1, and thus the streaming velocity of this gas.

Interaction and association between the molecular gas/H II complex and nonthermal Snake filament is also suggested by the data. First, the filamentary Snake terminates directly within the center of the G359.19−0.05 H II complex. There are no H II complexes of similar nature anywhere else along the extent of this serpent. Second, there is the distinct minimum in the CO emission where the filament crosses the perimeter of the surrounding molecular material. Moreover, both the molecular material and the filamentary Snake are known to be located in the Galactic center region; the molecular material is so deemed because of its high velocities and large line widths, and the nonthermal filament is defined by virtue of its 21 cm absorption-line observations (Uchida et al. 1992b). Of course, the previous points may simply detail a coincidental alignment between the filament and the cloud/H II region, rather than interaction between the two. The molecular "ring" is indeed clumpy in nature and has several minima in addition to that found where the nonthermal filament crosses its perimeter. In any case, if the superposition of the Snake with the molecular trough has a physical basis, it is unclear what it might be. Also, it is difficult to reconcile an anticoincidence between filament and molecular gas with the hypothesis of Serabyn & Morris (1994), who would predict that a molecular clump underlies each filament. One problem with G359.19−0.05 is that the filament has not yet been well characterized where it enters the H II region because of its faintness and therefore relatively low contrast. It may, for example, pass through the H II region and interact with a molecular clump on the western side. Regardless, the three-way coincidence among the molecular cloud, the H II region, and the nonthermal filament is notable, especially given the possible role that an H II region at the surface of a molecular cloud may play in the production or illumination of the filaments (Serabyn & Morris 1994).

4.2. *Clues for the Production Mechanism of the Galactic Center Filaments*

Is the association between an H II region lying at a molecular cloud surface and a nonthermal filament testament to the mechanism for producing the radio filaments in the Galactic center? All the radio filaments that have been sufficiently studied do seem to have cloud/H II region lying either at the end of the filament or at the position of a discontinuity along the filament.

The association between the "+25 km s^{-1}" molecular cloud and the linear filaments of the Galactic center radio arc is a well-established one. There, the +25 km s^{-1} cloud appears to have wrapped itself around the magnetic field lines defining the filaments, with its leading edge ionized either by a nearby external ionizing source, by the collision process, or by the combination of both. The velocities of the dense gas and of the ionized interface along the radio arc, as detailed from CS (Serabyn & Güsten 1991) and [Ne II] (Serabyn 1995) line observations, respectively, are consistent with the scenario of cloud flow around or into a local concentration of magnetic field lines.

Another candidate for a radio filament linked to a molecular cloud is the nonthermal filament G359.5+0.18, located just north of Sgr C. There a giant Galactic center molecular cloud is observed near one end of the filament (Bally, Yusef-Zadeh, & Hollis 1989). Interaction is implied by the data; where the cloud and the filament coincide, the filament bends smoothly to follow the perimeter of the molecular cloud.

The Sgr C region itself is a clear example of an association. The filament terminates within an H II complex and apparently near the surface of a molecular cloud (Liszt 1985; Liszt & Spiker 1995). Here the hypothesis of Serabyn & Morris (1994) can presumably be assessed by detailed examination of the molecular cloud lying at the endpoint of the filament. According to that hypothesis, the filament would originate at or near the ionized surface of a molecular clump.

The evidence presented here shows that the Snake filament may be another example supporting the hypothesis that a surfically ionized cloud moving at a relatively high velocity with respect to the ambient magnetic field provides the general means of illuminating the nonthermal filaments in the Galactic center via the conversion of magnetic energy

© American Astronomical Society • Provided by the NASA Astrophysics Data System

1996ApJ...462..768U

to particle energy. However, the H II region/molecular cloud complex which we have identified remains only a candidate source for the relativistic electrons in the Snake. The unusual kinks in the Snake offer other potential sites at which a molecular cloud may be responsible for discontinuities in the filaments, although if so, there is no thermal radio emission at those sites, and therefore, there is no obvious source of free electrons anywhere along the Snake except at its two ends. The problems with designating G359.1−0.55, the supernova remnant or superbubble at the southern end, as a source of electrons were discussed above.

Is the complex at the northern end a more likely source? The trend of spectral index along the Snake found by Gray et al. (1995) offers some support to this notion. The radio continuum spectrum is flat, or even slightly rising, near G359.19−0.05, and it generally steepens toward the southern end, although that trend is not monotonic. Thus, there is some indication that the electrons lose energy as they migrate from north to south along the Snake. Gray et al. (1995) argue that the synchrotron lifetime of $\sim 8 \times 10^5$ yr is comparable to the diffusion time for relativistic electrons along the entire length of the Snake, so that attribution of the steepening to energy loss is plausible.

A potential concern with the hypothesis that G359.19−0.05 is the energy source for the Snake is that the Snake is quite faint as it approaches this H II region. We speculate that this may be attributable to a varying magnetic field strength along the Snake; the kinks in this filament, for example, may correspond to locations at which the magnetic field lines have been both bent and compressed by the incursion of a local cloud. Inasmuch as the synchrotron emissivity depends on the local magnetic field strength, B, approximately as $B^{3/2}$, the intensity of the Snake filament should therefore increase toward the kinks, essentially as observed in the northwestern part of the Snake. So the faintness of the filamentary continuum emission at the northwestern extremity would thus be understood in terms of a relatively smaller magnetic field there.

In summary, we have found a molecular cloud/H II region complex which we suggest is the most likely source for the relativistic particles within the Snake filament. A more microscopic examination of the geometrical relationships among the filament, the molecular cloud, and the H II region is now needed to assess this hypothesis further.

The CSO is supported by NSF grant AST 93-13929.

REFERENCES

Anantharamaiah, K. R., Pedlar, A., Ekers, R. D., & Goss, W. M. 1991, MNRAS, 249, 262
Bally, J., & Leventhal, M. 1991, Nature, 353, 234
Bally, J., Stark, A. A., Wilson, R. W., & Henkel, C. 1987, ApJS, 65, 13
———. 1988, ApJ, 324, 223
Bally, J., Yusef-Zadeh, F., & Hollis, J. M. 1989, in IAU Symp. 136, The Center of the Galaxy, ed. M. Morris (Dordrecht: Kluwer), 189
Benford, G. 1988, ApJ, 333, 735
Bloemen, J. G. B. M., et al. 1986, A&A, 154, 25
Caswell, J. L., & Haynes, R. F. 1987, A&A, 171, 261
Echevarria, L. 1995, personal communication
Frerking, M. A., Langer, W. D., & Wilson, R. W. 1982, ApJ, 262, 590
Gray, A. D. 1994, Ph.D. thesis, Univ. Sydney
Gray, A. D., Cram, L. E., Ekers, R. D., & Goss, W. M. 1991, Nature, 353, 237
Gray, A. D., Nicholls, J., Ekers, R. D., & Cram, L. E. 1995, ApJ, 448, 164
Henkel, C., Wilson, T. L., Walmsley, C. M., & Pauls, T. 1983, A&A, 127, 388
Heyvaerts, J., Norman, C., & Pudritz, R. E. 1988, ApJ, 330, 718
Leahy, D. A. 1991a, IAU Telegram No. 5211
———. 1991b, MNRAS, 251, 22P
Lesch, H., & Reich, W. 1992, A&A, 264, 493
Liszt, H. S. 1985, ApJ, 203, 165
Liszt, H. S., & Spiker, R. W. 1995, ApJS, 98, 259
Mirabel, I. F., Morris, M., Wink, J., Paul, J., & Cordier, B. 1991, A&A, 251, L43
Mirabel, I. F., Rodriguez, L. F., Cordier, B., Paul, J., & Lebrun, F. 1992, Nature, 358, 215
Morris, M. 1990, in IAU Symp. 140, Galactic and Intergalactic Magnetic Fields, ed. R. Beck, P. P. Kronberg, & R. Wielebinski (Dordrecht: Kluwer), 361
———. 1995a, in Nuclei of Normal Galaxies: Lessons from the Galactic Center, ed. R. Genzel & A. Harris (Dodrecht: Kluwer), 185
———. 1995b, in IAU Symp. 169, Unsolved Problems of the Milky Way, ed. L. Blitz (Dordrecht: Kluwer), in press
Morris, M., Polish, N., Zuckerman, B., & Kaifu, N. 1983, AJ, 88, 1228
Morris, M., & Yusef-Zadeh, F. 1989, ApJ, 343, 703
Nicholls, J. 1992, Proc. Astron. Soc. Australia, 10, 128
Paul, J., et al. 1991, in Gamma Ray Line Astrophysics, ed. Ph. Durouchoux & N. Prantzos (New York: AIP), 17
Reich, W., & Schlickeiser, R. 1992, A&A, 256, 408
Serabyn, E. 1995, private communication
Serabyn, E., & Güsten, R., 1991, A&A, 242, 376
Serabyn, E., & Morris, M. 1994, ApJ, 424, L91
Sofue, Y. 1990, in IAU Symp. 140, Galactic and Intergalactic Magnetic Fields, ed. R. Beck, P. P. Kronberg, & R. Wielebinski (Dordrecht: Kluwer), 227
Tsuboi, M., Inoue, M., Handa, T., Tabara, H., & Kato, T. 1985, PASJ, 37, 359
Tsuboi, M., Inoue, M., Handa, T., Tabara, H., Kato, T., Sofue, Y., & Kaifu, N. 1986, AJ, 92, 818
Uchida, K. I., & Güsten, R. 1995, A&A, 298, 473
Uchida, K. I., Morris, M., Bally, J., Pound, M., & Yusef-Zadeh, F. 1992a, ApJ, 398, 128
Uchida, K. I., Morris, M., & Yusef-Zadeh, F. 1992b, AJ, 104, 1533
Wannier, P., 1989, in IAU Symp. 136, The Center of the Galaxy, ed. M. Morris (Dordrecht: Kluwer), 107
Yusef-Zadeh, F. 1989, in IAU Symp. 136, The Center of the Galaxy, ed. M. Morris (Dordrecht: Kluwer), 243
Yusef-Zadeh, F., & Bally, J. 1989, in IAU Symp. 136, The Center of the Galaxy, ed. M. Morris (Dordrecht: Kluwer), 197
Yusef-Zadeh, F., & Morris, M. 1987a, ApJ, 322, 721
———. 1987b, AJ, 94, 1178
Yusef-Zadeh, F., Morris, M., & Chance, D. 1984, Nature, 310, 557
Yusef-Zadeh, F., Paratharasan, P., Wardle, M., & Uchida, K. I. 1995, in IAU Symp. 169, Unsolved Problems of the Milky Way, ed. L. Blitz (Dordrecht: Kluwer), in press

© American Astronomical Society • Provided by the NASA Astrophysics Data System